

## 6. Discussion, conclusions and outlook

<b>Introduction.....</b>	<b>192</b>
<b>6.1 Discussion .....</b>	<b>193</b>
6.1.1 Ammonia detection.....	193
6.1.2 Hydrogen sulphide detection .....	204
6.1.3 Nitrogen dioxide detection .....	206
<b>6.2 Conclusions.....</b>	<b>208</b>
<b>6.3 Outlook .....</b>	<b>212</b>

### *Introduction*

As mentioned in Chapter 1, a multitechnique approach is necessary in order to understand the whole process of the detection of gases by MOX sensors. Basically, bulk and surface properties of the material (Chapter 3), electrical response to gases (Chapter 4) and superficial species and reactions (Chapter 5) have been analysed throughout this work. This last chapter aims at discussing the results previously presented as a whole, as well as presenting the main conclusions that can be drawn from this investigation and some proposals for a future research grounded on the present work. The correlation of the different results presented is often very complex and sometimes assumptions must be made in order to reason out the whole picture. This may lead to some tentative conclusions that probably need further investigations to be confirmed but that, at the same time, become an interesting point to progress in the understanding of these gas sensors. This chapter also includes the final conclusions and future outlook.

The chapter is divided into three main parts. Firstly, a discussion on the detection of the three main gases studied here is provided. The target is to correlate the information obtained from the surface reactions and species with the sensor response, taking into account the information about the structural properties of the material. Some of the points could have been presented in their corresponding chapter, but they are probably better understood after presenting the whole picture of the process. This section do not contain references at the end since it is assumed that it is based on the data and references presented in previous chapters (only new references are added as foot notes).

The second section contains the main conclusions that this research has led to. Finally, a proposal for future investigations on WO<sub>3</sub>-based materials for gas sensing applications is presented in the *Outlook* subsection.

## 6.1 Discussion

### 6.1.1 Ammonia detection

The information we have obtained from the interaction of ammonia with pure  $\text{WO}_3$  will be used as the general framework to understand the results of catalysed  $\text{WO}_3$ , so it is necessary to clarify the main points. As stated above, we will firstly proceed to analyse the surface species and reactions on pure  $\text{WO}_3$ . From DRIFTS experiments, it was clear that ammonia is adsorbed on Lewis and Brønsted acid centres. This point was confirmed by TPD experiments and both techniques suggest that ammonia more strongly adsorbed to Lewis centres at temperatures over  $200^\circ\text{C}$ . After being adsorbed, ammonia molecule undergo a series of reactions on pure  $\text{WO}_3$ , from which we know that:

- The intensity of the vibration of  $\text{W}=\text{O}$  centres falls off as ammonia is introduced at increasing temperatures. Nitrosil species appear on the surface of pure  $\text{WO}_3$  (DRIFTS experiments).
- The TPD products of ammonia are, apart from ammonia itself,  $\text{N}_2$ ,  $\text{N}_2\text{O}$ ,  $\text{NO}$  and  $\text{H}_2\text{O}$ , with the specific characteristics already discussed in Chapter 5.

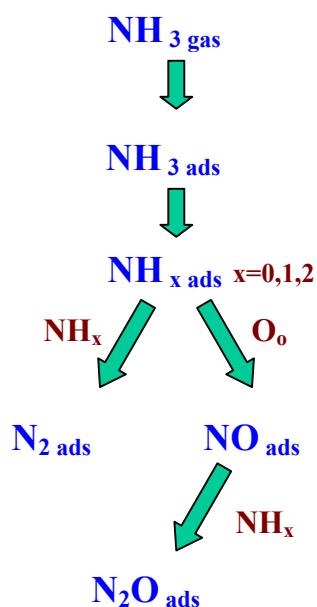


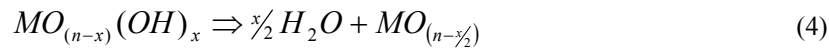
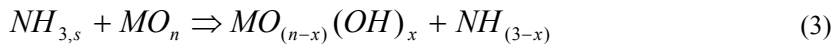
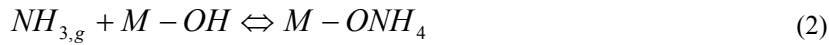
*Fig. 1:* Reaction paths for the oxidation of  $\text{NH}_3$

At this point, it is necessary to assume the following reaction path that was presented and argued in Chapter 5 and that is generally accepted in catalysis (Fig. 1). The ammonia molecule is firstly adsorbed on an acid centre. This is actually the first key point since ammonia is a strong base and so needs high valent acidic oxides, such as  $\text{WO}_3$ . This could be the first reason why this material is appreciated for ammonia detection. As soon the ammonia molecule is adsorbed, it can hop on the surface and thus undergo different processes. If it is not simply desorbed, the next step is its dehydrogenation through an oxygen species, which capture the hydrogen atom to form a hydroxyl group. This process leads to the formation of  $\text{NH}_x$  species, where  $x$  can have values of 2,1 or

## 6. Discussion, conclusions and outlook

---

0. These species are no longer likely to be desorbed but to further react following two main paths. They can interact with a second  $NH_x$  species to form molecular nitrogen ( $N_2$ ). The second option is that  $NH_x$  species react with an oxygen centre (either chemisorbed or lattice oxygen) to form nitrogen monoxide (NO). Furthermore, this NO can react with  $NH_x$  species to form nitrous oxide ( $N_2O$ ). This complex panorama, needless to say, admits many other reactions, with many contradictions in current literature (see references in Chapter 5). To sum up, the whole process could be described by the following reactions (some of them already presented)\*:



How are these features related to sensor response? Evidently, in order to have a variation of resistance, oxygen species must be consumed and this occurs through reactions (3)-(4) and (5). Actually, the formation of NO would apparently be much more convenient than the route leading to  $N_2$ , since more oxygen species are consumed. However, the main characteristic exhibited by gas sensors based on pure  $WO_3$  in this work concerning the detection of ammonia is their abnormal dynamic behaviour, which has been reported in Chapter 4. At that point, it was hypothesised that the interference of  $NO_x^-$  species could be the reason for this behaviour. DRIFTS measurements, presented in Chapter 5, apparently confirmed this point since nitrosil species appeared on the surface of pure  $WO_3$  after contact with ammonia at temperatures over room temperature. As a matter of fact, it has been reported that sensor response to NO by  $WO_3$  is not particularly high provided the atmosphere is inert. However, NO may easily be converted into  $NO_2$  in the presence of

---

\* *M is here representing a metal centre, which can be W or any other of the catalytic metals added if present. Besides, it must be understood that reaction (3) can occur in different steps and in different centres provided  $n > x$ , being  $x=3,2,1$ . Oxygen can be either chemisorbed species or lattice species.*

oxygen and, as it has been illustrated in Chapter 4,  $\text{WO}_3$  has a considerable sensor response to sub-ppm concentrations of these gas. This is an interesting point since many papers concerning the catalytic oxidation of ammonia do not take into account the presence of  $\text{NO}_2$ . In fact, this gas was not detected in TPD experiments but it must be remarked that, although the preadsorption is made in synthetic air, the following desorption is made in an inert atmosphere (without oxygen). In an oxygen-containing atmosphere, like that of DRIFTS experiments or test of gas sensors, the formation of  $\text{NO}_2$  is apparently likely.

Therefore, the enhancement of sensor response the addition of catalytic additives was expected to bring, was actually twofold: firstly, they should promote a more selective catalytic oxidation of ammonia in order to avoid undesired reaction products, e.g.  $\text{NO}$ ; secondly, they should improve sensor response to ammonia ( $R_{\text{AIR}}/R_{\text{NH}_3}$ ) through the consumption of more oxygen species. As to the first target, the selective oxidation of ammonia should ideally lead to nitrogen. Another option is the formation of nitrous oxide ( $\text{N}_2\text{O}$ ) (in situ or *internal* selective catalytic oxidation). As a matter of fact, gas sensors based on metal oxides have typically a low sensor response to  $\text{N}_2\text{O}$  and so it can not be considered that this gas would interfere on sensor response. However, its formation requires the presence of  $\text{NO}$  as an intermediate species, reaction (8), so the first selective oxidation route seems more appropriate. As regards the enhancement of sensor response, the additives used (transition metal ions) are extensively reported to undergo redox processes through the well-known Mars and van Krevelen mechanism\*. Of course, these oxidation-reduction of these centres should be able to be transduced into an electrical signal to the sensor by electrical sensitisation (Chapter 1). However, the formation of  $\text{NO}$  or  $\text{N}_2\text{O}$ , as cited above, would be more *efficient* in the reduction of these centres since more oxygen is consumed; at the same time, if more  $\text{NO}$  is produced, more chances to have an abnormal sensor response come out. How can these different effects be reconciled? Let's study each catalysed  $\text{WO}_3$ .

Concerning copper-catalysed  $\text{WO}_3$ , the first interesting point that must be noticed is the *actual* surface concentration of copper. XPS measurements revealed that the superficial ratio  $\text{Cu}/\text{W}$  was under 0.014. This low value confirms the DRIFTS results that indicated that ammonia molecules were mainly adsorbed on the same acid centres that in the case of

---

\* Briefly, the Mars and van Krevelen mechanism consider the oxidation of molecules on metal oxides as a two-step mechanism: (1) reaction between the reactant and the oxide to give oxygenated products and partially reduced metallic centres and (2) reoxidation of the centres with gaseous oxygen. (A. Bielanski, J. Haber, *Oxygen in catalysis*, Marcel Dekker Inc., New York (1991).

## 6. Discussion, conclusions and outlook

---

pure  $\text{WO}_3$ . However, as stated in Chapter 5, more ammonia molecules are adsorbed on copper-catalysed samples, according to the higher number of N-containing molecules desorbed in TPD experiments. Since XPS measurements showed the presence of reduced copper centres, probably Cu(I), these could be the acid centres needed to bond ammonia molecules since they can easily accept an electron.

As revealed by TPD data, when copper is present, there is a clear increase in the amount of  $\text{N}_2\text{O}$  desorbed, as well as a shift to lower desorption temperatures. This implies that copper centres catalyse the formation nitrous oxide. From the present data it is not possible to determine which are these *new* oxygen species that play a part to catalyse this reaction. It may be that ammonia-like species ( $\text{NH}_x$ ) react with oxygen species associated to copper with a binding energy lower than oxygen associated to tungsten centres. In fact, as cited in Chapter 1 and experimentally confirmed in Chapter 3 and 5, the surface of  $\text{WO}_3$  presents oxygen ions forming  $\text{W}=\text{O}$  centres, which is a rather strong bond. This is supported by the DRIFTS investigation, which showed no decrease in the intensity of the  $\text{W}=\text{O}$  vibration as ammonia was present. As a matter of fact, this feature was common to all the catalysed- $\text{WO}_3$  samples analysed, what supports that ammonia may react with oxygen species associated to the additives. As to  $\text{N}_2$ , the desorption peak of nitrogen remains at a similar temperature and with only a slightly higher value. At the same time, DRIFTS spectra illustrated no nitrosil species appeared after ammonia contact when copper was present. Assuming that  $\text{N}_2\text{O}$  should appear through the formation of NO, the adsorption-reaction mechanism of ammonia on  $\text{WO}_3:\text{Cu}$  might be:

- ammonia is mainly adsorbed on tungsten cations and probably on Cu(I) ions.
- some ammonia molecules probably react with chemisorbed oxygen on tungsten or copper centres and with oxygen bonded to Cu(II), reducing them to Cu(I), to form NO. The reaction with terminal oxygen of  $\text{W}=\text{O}$  bonds is avoided.
- some other ammonia molecules proceed as in pure tungsten oxide, being dehydrogenated  $\text{NH}_x$  species.
- a selective catalytic internal reaction is enhanced with copper addition, leading to the reaction of NO and  $\text{NH}_x$  to form  $\text{N}_2\text{O}$ . This partly avoids the presence of  $\text{NO}_x^-$  species on the surface. The oxidation to  $\text{N}_2$  is only slightly boosted.

Once the panorama of the superficial reactions of ammonia molecule seems to be clarified, how are these reactions influencing the sensor response? Fig. 2 displays the sensor resistance in air and the sensor response to 500 ppm of ammonia at  $200^\circ\text{C}$  as a function of

the XPS Cu/W superficial ratio for 700°C-annealed samples. In the case of WO<sub>3</sub>:Cu(0.2%), a ratio Cu/W of zero has been assigned as no copper was detected by XPS. Nevertheless, its presence is confirmed by EPR measurements (Chapter 3). The first striking feature of this plot is that sensor resistance increases with copper loading but in the case of WO<sub>3</sub>:Cu(5%). This trend is very similar for 400°C-annealed samples (see Chapter 4), what indicates this is not an accidental characteristic. In the case of 0.2-2% copper-catalysed samples, the increase of base resistance is really the effect needed to have electrical sensitisation, as explained in Chapter 1. Oxidised copper centres, specially if they are Cu(II), do create a

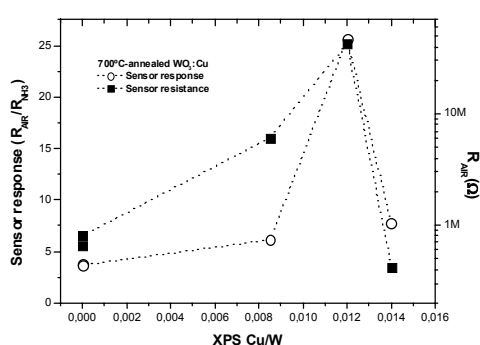


**Fig. 2:** Evolution of sensor resistance and sensor response of 700°C-annealed WO<sub>3</sub>:Cu with XPS Cu/W ratio.

greater depletion layer on WO<sub>3</sub> grains and thus a higher potential barrier between the grains. In fact, XPS revealed that the concentration of Cu(II) was clearly higher in the case of WO<sub>3</sub>:Cu(2%) than in the case of WO<sub>3</sub>:Cu(1%), what would account for the difference of resistance between both samples, apart from the increase in the total superficial copper content. As regards WO<sub>3</sub>:Cu(5%), once the distribution of copper on WO<sub>3</sub> has been analysed, it is clear that no copper-clustering was found by TEM at this concentration. Since surface concentration has similar values to 2 and 5% copper-catalysed samples, this may indicate that copper could have actually diffused into the WO<sub>3</sub> lattice and altered the number of electrons on the conduction band by a doping effect. Nevertheless, this is just a tentative proposal, being the reason rather obscure

Therefore, as Cu(II) centres near the contact between grains are reduced, this potential barrier should decrease and so *amplify* the sensor response. Actually, as noted above, the sample with the highest resistance in air, probably due to the highest concentration of Cu(II) centres, also exhibits the highest sensor response. Furthermore, WO<sub>3</sub>:Cu(2%) also showed a very low sensor response to NO<sub>2</sub>, specially compared to WO<sub>3</sub>:Cu(1%). Although there is a selective catalytic internal reaction of ammonia into N<sub>2</sub>O that reduces the presence of NO<sub>x</sub> species on the surface, this low sensor response to NO<sub>2</sub> also leads to a highest sensor response to ammonia. Therefore, these two factors make WO<sub>3</sub>:Cu(2%) a good candidate for ammonia detection: sensor response is enhanced through the reaction with oxygen centres probably associated to Cu(II) and sensor response to NO<sub>x</sub> is

## 6. Discussion, conclusions and outlook

---

minimised. On the other hand,  $\text{WO}_3:\text{Cu}(5\%)$ , which presents a similar TPD pattern and a moderate sensor response to  $\text{NO}_2$ , has in fact a low sensor response due to the absence of electrical sensitisation, as explained above.

As to vanadium-catalysed  $\text{WO}_3$ , it has been already noted that ammonia is mainly adsorbed on Brønsted acid sites, as revealed by DRIFTS studies and suggested by TPD data. These acid centres are probably V-OH related with the superficial vanadylic ions  $(\text{VO})^{2+}$  detected by EPR (Chapter 4). According to XPS data, the superficial V/W ratio is in this case as high as 0.133, nearly ten times higher than in the case of  $\text{WO}_3:\text{Cu}$ . This clarifies why adsorbed ammonia is detected on non-W sites in this case. As in the previous copper-catalysed samples, the amount of adsorbed ammonia is also higher than in pure  $\text{WO}_3$ , according to the desorption of N-containing species. This indicates that the addition of vanadium promotes the adsorption of ammonia. Moreover, since the amount of desorbed ammonia is similar to that of pure  $\text{WO}_3$ , it is clear that vanadium enhances the catalytic conversion of ammonia.

TPD revealed an interesting feature concerning the desorption of  $\text{N}_2$ . Although there was a single desorption peak, as for pure  $\text{WO}_3$ , this peak was displaced to lower temperatures as vanadium content increased, whereas the TPD area was maintained nearly constant. This suggests that the mechanism of  $\text{N}_2$  formation, being still the same that in pure  $\text{WO}_3$ , is catalysed by vanadium presence and so occurs with a lower activation energy. Assuming that  $\text{NH}_x$  species are the intermediate species that must recombine to form  $\text{N}_2$ , it may imply that, as more superficial vanadium centres appear, hydrogen abstraction needs lower activation energy and thus  $\text{NH}_x$  species can recombine more easily. As explained in Chapter 5, hydrogen abstraction requires the presence of oxygen ions to form hydroxyl groups, so vanadium centres must be active in reaction (3).

In much the same way as  $\text{N}_2$ , desorption peaks of  $\text{NO}$  and  $\text{N}_2\text{O}$  are also displaced to lower temperatures as vanadium concentration increases. Moreover, the desorption of these gases grows as vanadium content increases. As explained above, it is assumed that  $\text{NO}$  is formed through the reaction of  $\text{NH}_x$  with oxygen centres and that  $\text{NO}$  can further react with  $\text{NH}_x$  species to form  $\text{N}_2\text{O}$ . Obviously, vanadium centres are offering more oxygen centres available for reaction, probably with a lower V-O bond strength as vanadium concentration increases. This may be due to the formation of polymeric chains of  $\text{VO}_4$  units, which was suggested in Chapter 3. In fact, isolated vanadium centres present  $\text{V}=\text{O}$  bonds and these

bonds are stronger than V-O bonds in V-O-V chains, what would lead to a desorption at higher temperatures (higher activation energies).

To finish with the surface adsorption-reaction panorama of ammonia on vanadium catalysed  $\text{WO}_3$ , it must be borne in mind that neither consumption of oxygen on  $\text{W}=\text{O}$  centres, nor nitrosil species, were detected by DRIFTS studies. This means that oxygen species consumed by ammonia had weaker bindings than oxygen in  $\text{W}=\text{O}$  centres. These characteristics lead to the following picture of ammonia interaction with vanadium-catalysed  $\text{WO}_3$ :

- ammonia is adsorbed mainly on V-OH acid centres.
- some ammonia molecules are likely to react with oxygen centres associated to vanadium species, probably both  $\text{V}=\text{O}$  and  $\text{V}-\text{O}$ , as well as with chemisorbed oxygen, to form  $\text{NO}$ . The reaction with terminal oxygen of  $\text{W}=\text{O}$  bonds is avoided.
- vanadium centres promote the formation of dehydrogenated  $\text{NH}_x$  species with lower activation energy, leading to the desorption of  $\text{N}_2$  at lower temperatures.
- a selective catalytic internal reaction is produced, leading to the reaction of  $\text{NO}$  and  $\text{NH}_x$  to form  $\text{N}_2\text{O}$ . This reaction path is also catalysed by the addition of vanadium.

How are these features related with sensor response? Firstly, let's analyse the influence of vanadium addition on sensor resistance and on sensor response, for instance at  $200^\circ\text{C}$ . Fig. 3 displays these values as functions of XPS superficial vanadium concentration. This figure clearly indicates that as vanadium concentration increases, sensor resistance grows while the V/W ratio is under 0.1, decreasing beyond this point ( $\text{WO}_3:\text{V}(5\%)$ ). The evolution of the sensor resistance would suggest that, as expected, oxidised vanadium centres do create a

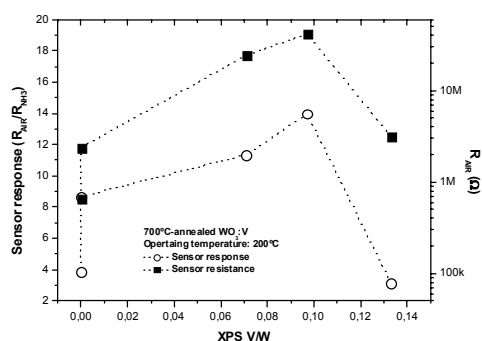


**Fig. 3:** Evolution of sensor resistance and sensor response of  $700^\circ\text{C}$ -annealed  $\text{WO}_3:\text{V}$  with XPS  $\text{V}/\text{W}$  ratio.

raise in the height of the intergrain potential barrier, in much the same way as copper-catalysed  $\text{WO}_3$ . However, as vanadium concentration is over a certain point, probably polymeric vanadium chains are formed, as suggested above, and these centres may not induce such an important depletion layer, leading to a certain decrease of sensor base resistance. More complex effects such as those mentioned above

## 6. Discussion, conclusions and outlook

---

for  $\text{WO}_3\text{:Cu}$ , concerning additive diffusion and change of carrier concentration, can not be ruled out either.

Interestingly, sensor response follows a similar trend to that of sensor resistance. Since a clear boost in catalytic activity appeared with increasing concentrations of vanadium, sensor response would be expected to increase too. However, in the case of  $\text{WO}_3\text{:V}(5\%)$ , sensor response is even lower than in pure  $\text{WO}_3$ . One tentative proposal to explain this discrepancy is that, although ammonia is oxidised, and so oxygen centres consumed, the electrical transduction of this phenomena seems to be minimised by the presence of polymeric vanadium chains. This would be similar to the effect of additive clusters that can oxidise in a very effective way but are not able to transduce this into an electrical signal. On top of that, the enhanced production of NO by vanadium presence could be another factor involved in the decrease of sensor response through the formation of  $\text{NO}_x^-$ , as extensively explained in Chapter 4.

Concerning chromium-catalysed  $\text{WO}_3$ , DRIFTS and TPD data revealed that adsorption centres of ammonia were basically those of pure  $\text{WO}_3$ . In fact, as chromium content increased, an apparent raise of ammonia desorbed from Brønsted centres is suggested from TPD data. This is in agreement with DRIFTS data, which showed a more intense and broader signal of  $\text{NH}_4^+$  at room temperature. Nevertheless, most ammonia is adsorbed on Lewis centres associated to  $\text{WO}_3$ . This is not surprising if XPS data are taken into account, since it was indicated in Chapter 4 that superficial Cr/W ratio was under 0.02 for 700°C-annealed samples. However, ammonia TPD peaks were typically so wide that contributions from chromium centres, either Lewis or Brønsted centres, should not be ruled out.

As already mentioned in Chapter 5, the most interesting characteristic of TPD of ammonia from chromium-catalysed samples is the appearance of multi-desorption peaks of nitrogen. This aspect, unique in the set of samples analysed in this investigation, is followed by a clear growth of desorbed nitrogen and of N-containing species in general. These new peaks suggest that chromium centres are highly active sites for ammonia dehydrogenation and thus  $\text{NH}_x$  species recombination. Cr=O centres could act as the Brønsted bases and become Cr-OH. In fact, the presence of more than one peak suggested that new mechanisms of  $\text{N}_2$  formation appear with chromium addition. Although reaction (7) proposed a complete dehydrogenation of the ammonia molecule in order to form  $\text{N}_2$ , some authors have

proposed alternative paths when chromium species are present<sup>\*</sup>, which might require lower activation energies. Besides, since these new peaks also appear at lower temperature, it means that chromium centres do catalyse the conversion of ammonia into nitrogen. It is interesting to notice again that the amount of desorbed nitrogen, from these new peaks and from the peak that already appear on pure  $\text{WO}_3$ , is well correlated with chromium content.

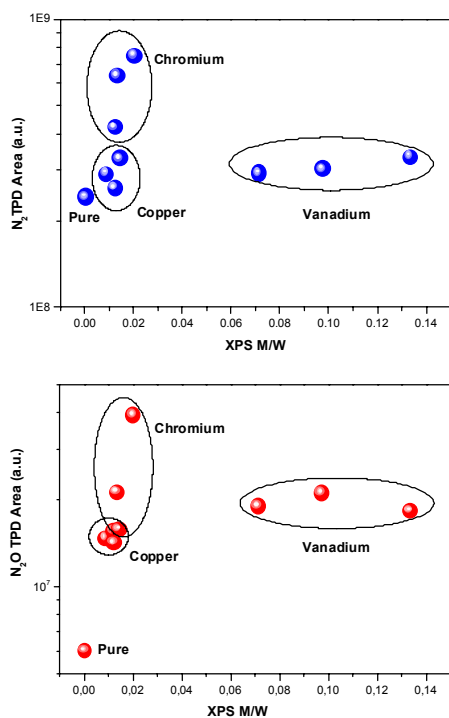


**Fig. 4:** TPD area of  $\text{N}_2$  and  $\text{N}_2\text{O}$  as functions of additive superficial concentration.

desorbed amount. As in the previous case of  $\text{N}_2$ , the desorption of nitrous oxide from chromium-catalysed  $\text{WO}_3$  was also clearly higher than from the other studied samples. This figures also illustrate an interesting point: whereas all three additives increase the desorption of  $\text{N}_2\text{O}$ , only chromium is able to produce a significant rise in  $\text{N}_2$  desorption. This feature might be related with the uniquely enhance of sensor response induced by this additive, as will be discussed below.

Therefore, these results suggest the following path for adsorption-reaction of ammonia on chromium-catalysed  $\text{WO}_3$ :

<sup>\*</sup> A. Baiker et al., *J. Catal.* 133 (1992) 397-414.

## 6. Discussion, conclusions and outlook

- ammonia is adsorbed mainly on tungsten centres, although adsorption on Lewis or Brønsted centres associated to chromium is also likely.
- chromium centres are very active in the formation and recombination of  $\text{NH}_x$  species to produce nitrogen, specially compared with the other catalytic additives tested and taking into account the real surface concentration. The activation of ammonia species could be done through  $\text{Cr}=\text{O}$  centres, although this is only a tentative proposal that is not confirmed yet. The appearance of new  $\text{N}_2$  desorption peaks suggest new mechanisms of ammonia oxidation into nitrogen.
- the selective catalytic internal reaction is also enhanced, leading to a rise in the reaction of  $\text{NO}$  and  $\text{NH}_x$  to form  $\text{N}_2\text{O}$ .

After presenting these characteristics, how might sensor response be explained? First of all, we can proceed as in the case of copper and vanadium by analysing the dependence of sensor response and sensor resistance on chromium content. Fig. 5 displays the sensor resistance in air and the sensor response to ammonia at  $225^\circ\text{C}$  as functions of XPS Cr/W ratio for  $700^\circ\text{C}$ -annealed  $\text{WO}_3:\text{Cr}$ . It is evident that sensor resistance rises more than 2 orders of magnitude as chromium is added to  $\text{WO}_3$ . It is necessary to mention that  $\text{Cr}_2\text{O}_3$  is a p-type semiconductor, what may lead to think that in this case we have p-n junctions that induce high resistance barriers. However, considering the characterisation of chromium centres illustrated in Chapter 3, it is doubtful that  $\text{Cr}_2\text{O}_3$  is formed, being dispersed

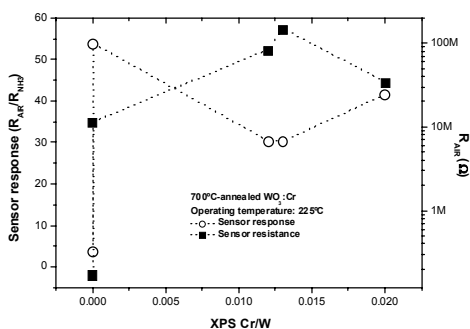


**Fig. 5:** Evolution of sensor resistance and sensor response of  $700^\circ\text{C}$ -annealed  $\text{WO}_3:\text{Cr}$  with XPS Cr/W ratio

chromium species much more likely. However, formation of this oxide can not be completely ruled out. Interestingly, sensor resistance slightly diminishes as chromium content is introduced in a nominal concentration of 5%. This effect can be related to a similar decrease in  $\text{Cr}=\text{O}$  Raman intensity vibration already mentioned in Chapter 3, where a formation of polychromate species was suggested to explain this reduction.

As regards sensor response, at least two interesting features need some explanations: why sensor response increases so much with the addition of chromium and why this sensor

response is higher for  $\text{WO}_3:\text{Cr}$  than for the rest of samples. As for the first question, Fig. 4 has already displayed the high catalytic activity of chromium-catalysed  $\text{WO}_3$ . Moreover, the key point might probably be the boost to  $\text{N}_2$  desorption that induces chromium addition, even in a very low concentration. This is suggested by the comparison of  $\text{N}_2$  TPD area and sensor response between copper, vanadium and chromium-catalysed samples (Fig. 6). This

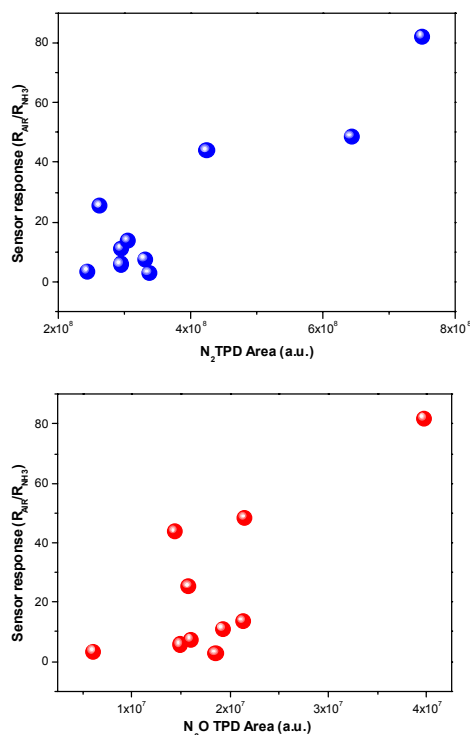


**Fig. 6:** Correlation between sensor response to ammonia (500 ppm at 200°C) and TPD areas of  $\text{N}_2$  and  $\text{N}_2\text{O}$ .

figure indicates that the production of  $\text{N}_2$  might be correlated with sensor response. Moreover, it is suggested it is actually the appearance of a  $\text{N}_2$  desorption peak at lower temperatures in  $\text{WO}_3:\text{Cr}$  what indicates an effectively catalytic power of chromium centres, and not only the amount of  $\text{N}_2$  desorbed. This is the selective catalytic oxidation of ammonia to nitrogen that is required to avoid  $\text{NO}$  interference. On the other hand, the correlation between  $\text{N}_2\text{O}$  desorption and sensor response is not so straightforward. It is necessary to remember again that desorption of gases in TPD experiments was made in an inert atmosphere, what means that  $\text{NO}$  molecules had low chances to be further oxidised into  $\text{NO}_2$  and recombination with  $\text{NH}_x$  species to form  $\text{N}_2\text{O}$  appears more probable. In fact, this argument

could be used to understand why sensor response falls off with higher chromium content than 0.2% and finally increases with  $\text{WO}_3:\text{Cr}(5\%)$ . As TPD data suggest, when chromium content increases, more oxygen centres are able to react to finally form  $\text{N}_2\text{O}$ ; however, sensor response was adversely affected. This was in fact true for the rest of additives tested: an increase of additive content led to a highest amount of desorbed  $\text{N}_2\text{O}$  but not always to a rise in sensor response. The reason might be that two competitive effects might occur: more oxygen centres are consumed (reduction of resistance) and more  $\text{NO}_x$  species are produced (rise of resistance), as  $\text{NO}$  must precede the formation of  $\text{N}_2\text{O}$ . In other words,  $\text{N}_2\text{O}$  production and sensor response are not easily correlated due to the interference of  $\text{NO}$ .

## 6. Discussion, conclusions and outlook

### 6.1.2 Hydrogen sulphide detection

One of the most interesting features presented concerning hydrogen sulphide detection by gas sensors based on pure  $\text{WO}_3$  was the extremely important interference of humidity. Although TPD measurements were performed in dry air, these data can give us the clue of these phenomena. As already stated in Chapter 5, hydrogen sulphide can be both dissociatively and undissociatively adsorbed on  $\text{WO}_3$ . For gas sensing applications, only the dissociative adsorption is apparently interesting, since molecularly adsorbed hydrogen sulphide is not on the surface over  $100^\circ\text{C}$ . As already mentioned in Chapter 5, this dissociation leads to proton ( $\text{H}^+$ ) and sulfhydryl ( $\text{HS}^-$ ) species. Therefore, this dissociation must take place on strong acid-base pair sites, so as to form  $\text{H}^+$ -basic site and  $\text{SH}^-$ -acid site\*. Basically, superficial OH and SH species will appear and SH are the active species that will react with oxygen centres, as revealed by TPD measurements.

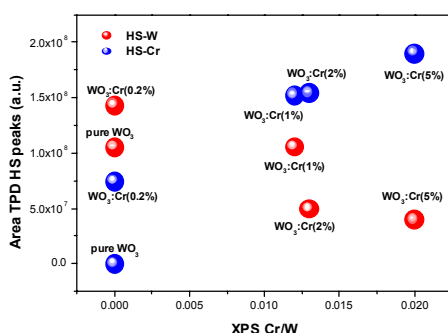


**Fig. 7:** TPD HS-area as a function of XPS Cr/W ratio.

Therefore, sensor data indicate that a competition between these two dissociative reactions occur, what leads to an effective lower sensor response to hydrogen sulphide in humid air.

Regarding catalysed  $\text{WO}_3$ , the most interesting results were obtained with chromium catalysed  $\text{WO}_3$ , as they showed an improved sensor response compared to pure  $\text{WO}_3$ . TPD studies showed an interesting feature concerning this material: a second adsorption site for SH groups was available as chromium was added. Actually, not only the number of HS species increases, but also the new site becomes dominant, as displayed in Fig. 7, where the area of both peaks is plotted after peak deconvolution. In this figure the peaks have been

\* See Appendix 2 for a brief explanation of acid-basic sites on metal oxides.

labelled as HS-W (the one that is present in pure and chromium catalysed  $\text{WO}_3$ ) and HS-Cr (the second peak that appears in  $\text{WO}_3:\text{Cr}$ ). Since the area of this second peak is correlated with the concentration of superficial chromium centres, it is possible to speculate that this new centre is either on Cr ions or in W centres in the vicinity of chromium species. In fact, chromium addition not only induces a growth of desorbed  $\text{H}_2\text{S}$ , but also of  $\text{SO}_2$ , as

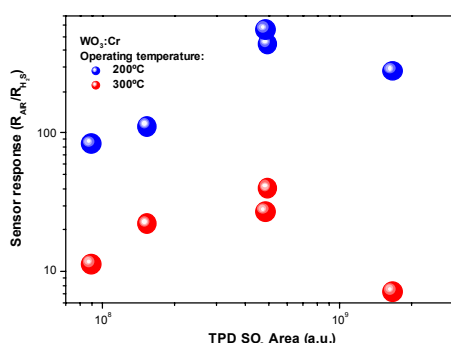


**Fig. 8:** Sensor response of  $\text{WO}_3:\text{Cr}$  as a function of TPD  $\text{SO}_2$ -area.

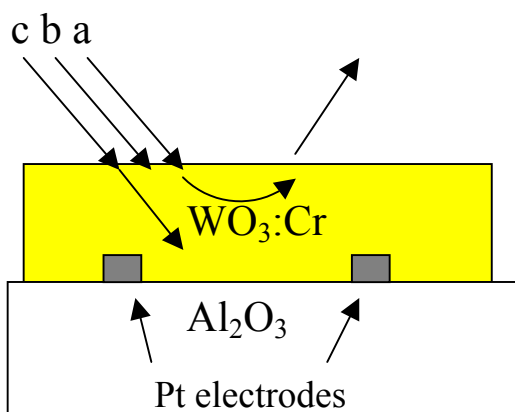


**Fig. 9:** Schema of influence of catalytic activity on sensor response: a) too high catalytic activity, b) low catalytic activity and c) appropriate catalytic activity.

mentioned in Chapter 5. These facts indicate that chromium addition enhances the dissociation of hydrogen sulphide and its reaction with oxygen species, probably associated with chromium centres.

Fig. 8 displays the sensor response to 20 ppm of  $\text{H}_2\text{S}$  (operating at 200°C and 300°C) as a function of the TPD  $\text{SO}_2$  area (after adsorption at room temperature). This value of the TPD area is interpreted as a measurement of the catalytic activity of the sample to convert hydrogen sulphide into sulphur dioxide. In Chapter 5 it was illustrated that this TPD  $\text{SO}_2$  area raises as chromium content increases. It is evident from this figure sensor response is maximised for 1-2% chromium catalysed samples, whereas sensor response decreases as chromium content increases. This effect is typical of thick films based on catalysed metal oxides and is called *configurational effect*<sup>\*</sup> (see Figure 9<sup>\*\*</sup>). In fact, there is a fundamental difference between the sensor thick-film and the sample used for TPD measurements. Briefly, the sensor film is porous and thus gas can diffuse through the whole layer. However, since this gas is consumed, there will be different permeation amounts in the inner parts of the layer depending on the catalytic activity. If the sensing material has a

<sup>\*</sup> Y. Shimizu, M. Egashira, *MRS Bulletin* (June-1999) 18-24.

<sup>\*\*</sup> Adapted from Yamazoe et al., *J. Molec. Catal. A* 155 (2000) 193-200.

## 6. Discussion, conclusions and outlook

very high catalytic activity (e.g.  $\text{WO}_3\text{:Cr}(5\%)$ , case *a*), most of the gas (hydrogen sulphide in our case) will be consumed in the outermost region of the sensing film, being unable to induce a resistance change throughout the whole layer. If the activity is rather low (e.g. pure  $\text{WO}_3$ , case *b*), sensor response will be moderate. With intermediate values of catalytic activity (e.g.  $\text{WO}_3\text{:Cr}(1\text{-}2\%)$ , case *c*), target gas can penetrate through the whole layer and so induce larger resistance changes. On the other hand, TPD samples are pressed into discs and then crushed into granules to avoid this sort of diffusion effects.

Finally, test of these sensors also revealed a significant rise in sensor recovery after  $\text{H}_2\text{S}$  detection in sensors based on  $\text{WO}_3\text{:Cr}$  compared to those based on pure  $\text{WO}_3$  (Fig. 10). As

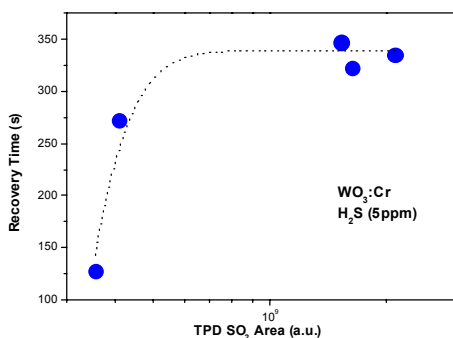


**Fig. 10:** Dependence of recovery time with TPD  $\text{SO}_2$ -area for  $\text{WO}_3\text{:Cr}$ .

the target gas is purged with air in test measurements, oxygen must refill those sites where it was previously adsorbed and sensor resistance must recover its initial value. However, oxidation products must desorb in order to *free* the sites occupied. TPD data revealed that, as adsorption temperature increased from room temperature to  $200^\circ\text{C}$ , the amount of desorbed  $\text{SO}_2$  grew. This fact suggests that the desorption of sulphur dioxide might be a key point for sensor recovery. Fig. 8 displays the evolution of recovery time\* (operated at  $200^\circ\text{C}$ , 5 ppm of  $\text{H}_2\text{S}$ ) with the amount of  $\text{SO}_2$  desorbed at  $200^\circ\text{C}$ . This figure suggests an exponential dependence of recovery time with TPD  $\text{SO}_2$  area.

### 6.1.3 Nitrogen dioxide detection

Regarding pure  $\text{WO}_3$ , in addition to an obvious difference of mean grain size and crystalline quality between materials annealed at  $400^\circ\text{C}$  and  $700^\circ\text{C}$ , structural differences have to be taken into account to explain differences on sensor response. As already stated in Chapter 4, gas sensors based on  $700^\circ\text{C}$ -annealed  $\text{WO}_3$  showed a higher sensor response to  $\text{NO}_2$  than those based on  $400^\circ\text{C}$ . In fact, Yamazoe et al. have already stated that the correlation sensor response-grain size in the case of  $\text{NO}_2$  detection by  $\text{WO}_3$  is not so

\* Recovery time was evaluated as the time that  $(R_{\text{AIR}} - R_{\text{H}_2\text{S}}) / R_{\text{H}_2\text{S}}$  takes to reach from 90% to 10% of the total value.

straightforward as: *the smaller the grain size is, the higher sensor response gets*. As a matter of fact, after reviewing the results presented in chapter 4, this might also be true for ammonia and hydrogen sulphide detection. Surface defects and configuration seem to play a key role on the detection. For instance, it has been reported that high annealing temperature leads to better NO<sub>2</sub> sensor response, despite grain size increase, in screen-printed gas sensors based on SnO<sub>2</sub> nanopowders. This was attributed to the improvement of the crystalline quality and the faceting of nanograins, which improved NO<sub>2</sub> adsorption. since there was not a clear correlation between

As revealed in Chapter 3, near-surface oxygen deficiencies, with their associated crystalline shear planes, were present in 400°C-annealed WO<sub>3</sub>. These defects were present even at operating temperatures of 300°C, as indicated by XRD measurements under controlled temperature. However, they gradually disappeared as annealing temperature increased over 400°C, being apparently eliminated after the 700°C-annealing. This may reflect that oxygen deficiencies may drift to the surface of the grain and become reactive sites for the chemisorption of NO<sub>2</sub><sup>-</sup>. Nevertheless, more spectroscopic in-situ measurements are requested in order to confirm this hypotheses, which may explain reported differences on sensor response.

As to catalysed WO<sub>3</sub>, copper-catalysed WO<sub>3</sub> showed the highest sensor response to NO<sub>2</sub>. As confirmed in Chapter 3, this additive was not mainly oxidised to its highest value, and so copper centres, specially Cu(I), were available to donate electrons for the chemisorption of NO<sub>2</sub>.

### 6.2 Conclusions

This dissertation has examined the structural, vibrational and gas sensing properties of pure and catalysed WO<sub>3</sub> nanocrystalline powders, as well as the species and reactions that occur on their surface. This study has led to the following conclusions:

- Nanocrystalline tungsten oxide was obtained from tungstic acid by a chemical route, with a grain size between 15 nm and 120 nm (obtained by TEM), depending on the annealing temperature (between 400°C and 700°C).
- Crystalline structure of 400°C-annealed WO<sub>3</sub> was mainly triclinic, as revealed by Raman spectroscopy. As annealing temperature increased, monoclinic structure appeared, leading to coexistence of both structures in 700°C-annealed WO<sub>3</sub>. These structures were stable at usual operating temperatures of the sensor.
- Crystalline shear planes appeared in 400°C-annealed WO<sub>3</sub>, according to TEM investigations. XRD simulations were performed in order to include this defect and fit experimental XRD spectra. These simulations allowed following the evolution of the concentration of these defects, revealing that they disappear after the 700°C-annealing. High-temperature XRD spectra indicated that these defects are stable in 400°C-annealed WO<sub>3</sub> up to 300°C.
- Crystallite size and grain size and shape is not considerably affected by the addition of copper, vanadium and chromium using this experimental procedure.
- According to XRD data, additives neither formed a separate crystalline phase nor produced noticeable distortions of the WO<sub>3</sub> bulk crystalline phase. On the other hand, main Raman WO<sub>3</sub> vibration was affected by additive addition, as revealed by the FWHM. This may indicate that additives do diffuse to the bulk and, at least, the outermost layers of tungsten oxide are slightly distorted.
- Copper was present on the surface of particles as Cu(II) and, mainly, as reduced copper, probably Cu(I), according to XPS data. EPR revealed that Cu(II) were well distributed on WO<sub>3</sub> as their concentration was low and that copper ions approached as annealing temperature increased.
- TEM-EELS characterisation indicated that vanadium was well distributed (without forming clusters) on WO<sub>3</sub>. Vanadium centres were mainly V(V), with V(IV) also present in a small percentage, according to XPS data. V(IV) centres were detected by EPR, showing that they can be as V<sup>4+</sup> (bulk) and VO<sup>2+</sup> (surface).

- Raman investigations revealed that Cr=O vibrations were present in chromium catalysed samples, probably due to monochromate superficial species. Chromium centres were well distributed on WO<sub>3</sub>, according to TEM-EELS investigation. Surface chromium centres were mainly Cr(III), although Cr(V) was present in as prepared and 400°C-annealed samples.
- Pure WO<sub>3</sub> was not suitable for the detection of ammonia in the range of 20 to 500 ppm of NH<sub>3</sub> in synthetic air due to abnormal sensor resistance behaviour. 700°C-annealed WO<sub>3</sub> shows a better sensor response to H<sub>2</sub>S in dry synthetic air than 400°C-annealed WO<sub>3</sub>. It was found that sensor resistance in H<sub>2</sub>S atmosphere increases as humidity is present, leading to a lower sensor response. Sensor response to hydrogen sulphide of 400°C-annealed material is less influenced by the presence of humidity. 700°C-annealed WO<sub>3</sub> shows a better sensor response to NO<sub>2</sub> in dry synthetic air than 400°C-annealed WO<sub>3</sub>. 700°C-annealed pure WO<sub>3</sub> also presents a lower dependence with humidity since sensor resistance in synthetic air or NO<sub>2</sub> atmospheres is not highly dependent on humidity.
- 700°C-annealed WO<sub>3</sub>:Cu(2%) presented a suitable dynamic behaviour at 200°C. Besides, it presented a good sensor response to NH<sub>3</sub> in the range from 20 to 500 ppm and a low interference from humidity. Gas sensors based on 400°C-annealed WO<sub>3</sub>:Cu(2%) showed an improved sensor response to hydrogen sulphide with low interference from humidity in the range 30-80% relative humidity. High sensor response to NO<sub>2</sub> was achieved when copper was introduced in 1% atomic percentage. However, dynamic behaviour was not completely satisfactory in the range of NO<sub>2</sub> concentration analysed.
- Some of the gas sensors based on vanadium catalysed WO<sub>3</sub> still presented an abnormal sensor response to ammonia, similar to that previously reported for pure WO<sub>3</sub>. 700°C-annealed WO<sub>3</sub>:V(2%) presented a normal dynamic behaviour throughout the range of temperatures tested. Particularly, sensor response to ammonia at 300°C was interesting due to its fast sensor recovery. Sensor response to hydrogen sulphide decreased as vanadium was introduced, revealing that these sensors are not interesting for H<sub>2</sub>S detection.
- Chromium addition significantly increases the sensor response to ammonia. Sensors based on WO<sub>3</sub>:Cr(0.2%) exhibited a high sensor response to ammonia combined with a fast sensor recovery. Chromium addition also enhances the sensor response to hydrogen sulphide, specially at low temperatures. The maximum sensor response was

## 6. Discussion, conclusions and outlook

---

achieved when chromium was introduced in 1-2% atomic concentrations and operated at 200°C.

- Two different kinds of water are adsorbed on the surface of the powders at room temperature, according to DRIFT results. One species is desorbed as temperature is risen over room temperature, while the other one is not desorbed until the temperature is over 200°C in synthetic dry air. Two different kinds of hydroxyl groups are adsorbed on the surface of the powders at room temperature too, according to DRIFT results. In this case, one species decreases as temperature is above room temperature, whereas the other one is stable up to 400°C.
- Ammonia adsorption revealed that two different acid sites are present on the surface of  $\text{WO}_3$  following DRIFT measurements: Lewis and Brønsted acid sites. This fact is confirmed by TPD of ammonia, since it presents two peaks that are attributed to ammonia on these different sites. Ammonia on Brønsted acid sites (OH groups) desorbs at temperatures on 200°C. Only vanadium catalysed  $\text{WO}_3$  exhibits strong Brønsted acidity, as concluded from both DRIFT and TPD experiments. There are at least two different Lewis acid sites (unsaturated cations) in the examined  $\text{WO}_3$  powders and ammonia is stable in one of them up to 300°C.
- On pure  $\text{WO}_3$ , ammonia is apparently reacting with oxygen species belonging to terminal W=O bonds as DRIFT measurements show. Besides, nitrosyl species are also detected, probably coming from adsorbed NO. These features are not found in catalysed  $\text{WO}_3$ , what may indicate that additives prevent this reaction from happening.
- The previous point is clarified by TPD measurements, that revealed fundamental differences in the desorption of ammonia-oxygen combustion products (nitrogen, nitrous oxide, nitrogen monoxide and water). According to TPD data and assuming the reaction mechanisms explained above, it is proposed that more sites for  $\text{NH}_x$  species are available when additives are present. Moreover, ammonia reacts with other oxygen species than terminal W=O groups, tentatively oxygen species associated to the additives. As the concentration of  $\text{NH}_x$  species is high, the reaction of NO with one of this species to form  $\text{N}_2\text{O}$  is enhanced and so NO is less present on the surface, what may account for the DRIFT data.
- Remarkably, chromium addition leads to nitrogen desorption at low temperatures, reflecting that a high concentration of  $\text{NH}_x$  reactive species appear when chromium is present. Besides, these new  $\text{N}_2$  peaks suggest the presence of alternative oxidation paths of ammonia into nitrogen and may account for the high sensor response to ammonia exhibited by gas sensors based on  $\text{WO}_3\text{:Cr}$ .

## 6. Discussion, conclusions and outlook

---

- Hydrogen sulphide is both undissociatively and dissociatively adsorbed on pure and chromium catalysed  $\text{WO}_3$ , although only HS species are found over  $100^\circ\text{C}$ . The combustion products desorbed are sulphur dioxide and water
- Chromium introduction provides a new adsorption site for SH species, apparently contributing to the dissociation of hydrogen sulphide. Moreover, chromium addition leads to enhance the catalytic combustion of hydrogen sulphide, although more  $\text{SO}_2$  is adsorbed.

## 6. Discussion, conclusions and outlook

---

### 6.3 Outlook

Many avenues for further research remain for extending the current work, some of which are suggested and described below:

- It would be interesting to reduce the grain size under 20 nm in order to improve sensor response. One strategy could be to synthesise tungstic acid instead of using a commercial one, since this would allow a greater control on the initial properties of the material.
- The method of addition of catalytic additives could be improved so as to make it more effective. It could be interesting to impregnate annealed  $\text{WO}_3$  with the precursors of these additives and compare this route with the one used here. A better characterisation of these additives is needed, probably by using XPS with a pretreatment chamber or by using EPR in much more detail.
- The stability of the obtained sensors should be confirmed by long tests under real working conditions. Longer annealing treatments should be also explored in order to achieve high stability.
- The test of micromachined gas sensors based on these powders merits further investigations, specially the use of pulsed heating.
- DRIFTS and TPD studies should be extended to different gases in dry and humid conditions.
- Studies on catalytic activity at different operating temperatures are highly required.